https://doi.org/10.20965/jrm.2004.p0104

Paper:

Development of Horse-Type Quadruped Robot (Report2, Experiments of Trot Gait by Quadruped Robot PONY)

Shinobu Makita, Daisuke Nishimura, and Junji Furusho

Department of Computer-Controlled Mechanical Systems, Osaka University
2-1, Yamadaoka, Suita-shi, Osaka 565-0871, Japan
E-mail: furusho@mech.eng.osaka-u.ac.jp

[Received February 28, 2003; accepted May 12, 2003]

In this paper, we studied the equine gait, focusing on trotting, to realize a horse-type trot using a quadruped robot. Mammals use energy stored in the tendons during supporting phase. The change of angle in the equine fetlock stretches the tendons, storing energy. Fetlock movement is passively controlled by tendons, not actively controlled by muscles. We developed an equine quadruped robot, which uses actuators consisting of a serially connected motor and spring corresponding to equine muscles and tendons, e.g., the superficial digital flexor muscle. In this paper, we discuss simulation experiments showing the effectiveness of the motor-spring system, then PONY's horse-like trot.

Keywords: quadruped robot, horse-type robot, trot, tendon, spring

1. Introduction

Many studies of quadruped robots have conducted [2-19]. Among these studies, following have achieved a dynamically stable gait. In the mid-1980s, Reibert et al. achieved trotting, pacing, and bouncing using a hopping robot with four telescopic legs driven by hydraulic actuators with all four legs simultaneously in the swinging phase [3]. Miura et al. studied trotting and pacing using the articulated quadruped robots COLLEY-1 and COLLEY-2 [4,5].

In the 1990s, Hirose and Yoneda et al. studied gait shifting from a crawl to a trot, dynamic and static fusion gaits, etc. [6,7]. Emura et al. [8], Sakakibara and Kan et al. [9], and Takita and Seto [10] proposed using a reaction fly-wheel for controlling the trot in a lower impact trajectory and using actuators for the ankles.

Kimura et al. used a neural oscillator for dynamically stable pacing and trotting [11] and a dynamically stable gait on irregular terrain [12]. They recently introduced a spinal reflex mechanism through a central pattern generator for autonomous biologically inspired adaptive dynamic walking on moderately irregular terrain [13].

In quadruped robot gaits using passive joints [14,15], Furusho and Sano et al. realized gait shifting from a crawl to a trot, bounce, etc., using a quadruped robot [16-18]. Takeuchi [19] studied a horse-type quadruped robot.

Dynamically stable gaits using quadruped robots are basically achieved by making robot leg trajectories based on an engineering approach. Our aim is to reveal mechanism of mammalian walking based on articulated robot control. The purpose of this study is to analyze the equine limb structure and to develope a horse-type robot whose gait was controlled using equine gait data analysis - points that differ from conventional studies in robot engineering.

We previously proposed a walking model [24] based on equine data and developed a quadruped robot, PONY, using elastic energy stored in soft tissue, such as tendons, that passively generates movement and its control system.

In this paper, we report the simulation of trotting and the results of gait control experiments using PONY. First, we made a gait simulator of PONY, then conducted simulation experiments on PONY's gait using control based on equine walking. Simulation results showed that a dynamically stable gait could be realized with PONY. Finally, we conducted gait experiments using the same control and reference trajectories as used for simulations and realized a dynamically stable trot. Reference trajectories in simulations and experiments are based on an equine trot.

2. Walking System and Horse-type Quadruped Robot PONY

2.1. Model of Walking System

Figure 1 shows the equine skeleton and joints important to constructing a walking system. For simplicity and to make the system lightweight, we proposed a headless and neckless model focusing on limb movement in a trot, especially fetlock movement. In gait analysis, bones considered to move as one part were treated as one link, so the proposed model consisted of a one-link body and 4 legs, each consisting of 4 links.

We adopted a closed link (**Fig.2**) that interlocks

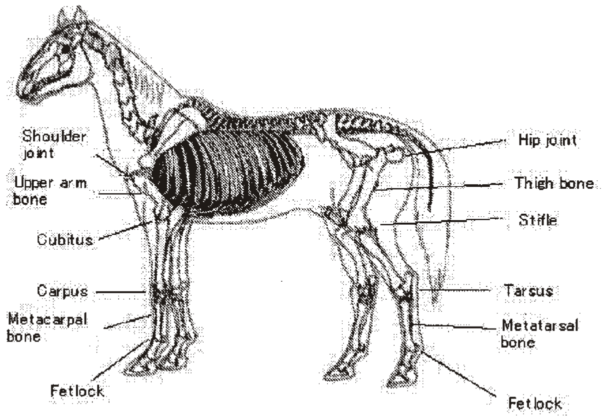

Fig. 1. Equine skeleton [20].

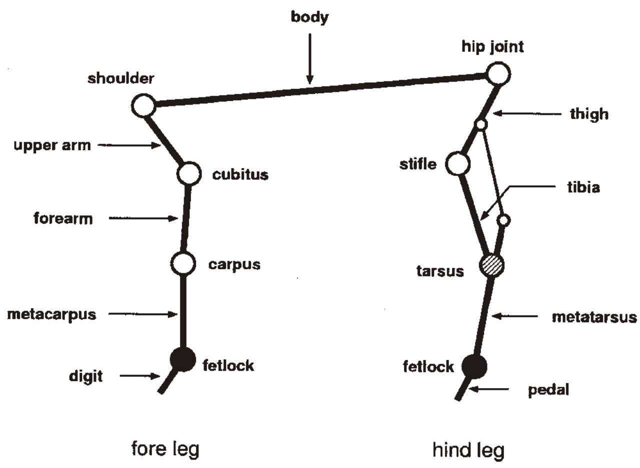

Fig. 2. Model of walking system; Lateral view.

movement of the stifle (the knee-like joint above the equine hock in the back leg) and tarsus (ankle) to reduce the number of motors and speed reducer for lightweight construction. Joints marked with large white circles in **Fig.2** are motor-driven and those marked with black circles use a drive consisting of a serially connected motor and spring with the tarsus (hatched circles) interlocked with the stifle. Although the equine shoulder and hip are triaxial, their main movement is back and forth, so we treated them as monoaxial. Other joints are monoaxial hinges [21], so all joints of the proposed model have a single degree of freedom, i.e., rotation around the pitch axis.

2.2. Muscle and Tendon Model in Fetlock Drive

We used a motor as the muscle actuator and a spring as the tendon's elastic element at the fetlock. We used a serially connected motor and spring because the digital flexor muscle has a long tendon at one end, and structurally acts as a serially connected actuator and elastic element.

2.3. Horse-type Quadruped Robot PONY

We designed and fabricated PONY, a horse-type quadruped robot with aluminum alloy links, based on the proposed model (**Fig.3**). PONY weighs 30[kg] and is 0.9[m] long, 0.63[m] high, and 0.51[m] wide. Each link is about one-third the length of the horse used in trot analysis. We adopted a closed link for the hind leg. Thus, the foreleg has 4 driven joints and the hind leg 3. We used DC servomotors (L406-011EL9 (60 W) Sanyo Denki Co., Ltd.) for actuators and gear trains and a timing belt and pulley (Mitsuboshi Belting Ltd.) for speed reduction. PONY has a drive consisting of a serially connected motor and spring at the fetlock.

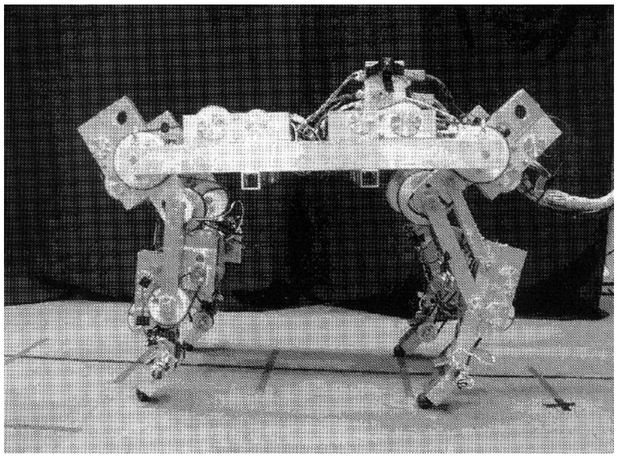

Fig. 3. Horse-type quadruped robot PONY.

2.4. Mass Distribution of Horse and PONY

Table 1 shows the mass in a thoroughbred divided into 5 sections and their percentage to total mass (average of 3 horses) together with the mass and percentage corresponding to each section of PONY.

Table 2 compares the horizontal center of mass (CM) of a horse from the literature [21] and CM of PONY on the sagittal plane. These show the percentage of length from shoulder to CM along the body.

Most of the equine mass is distributed in the body and only about 6% of total mass is distributed in the limbs. For PONY, leg mass occupies about 63% of total mass. The equine CM is about 36% of the length from the front of the body because of the mass of the head and neck, whereas the CM of PONY is about 46% of the length from the front of the body. The links of PONY are about one-third the equine length but mass distribution differs due to limits on the output/weight ratio of actuators.

Table 1. Weight and percentage.

	Weight of horse		Weight of robot	
	$[kg]$	$[\%]$	$[kg]$	$[\%]$
Head and neck	57.7	11.4	—	—
Trunk and tail	415.9	82.5	11.062	37.35
Total forelimbs	14.2	2.8	10.33	34.88
Total hindlimbs	16.3	3.3	8.228	27.78
Total weight	504.3	—	29.62	—

Table 2. Position of center of mass (Percentage from shoulder joint).

Horse	Robot
36	46

3. Sumulator

3.1. Modeling

For trot experiments using PONY, we conducted simulation experiments. For simplicity, we assumed the following:

Assumption 1: In the trot, legs on a diagonal line are synchronized and rotational moment around supporting legs is almost canceled by changing supporting legs.

Under this assumption, trotting was modeled as a 2-dimensional movement on the sagittal plane.

For contact between the legs and floor, we assumed the following:

Assumption 2: After contacting the floor, the leg does not slip but is fixed at that point.

Coefficients in the simulation are shown in **Tables 3-5**. l_i is the length of the i-th link, m_i is the mass of the i-th link, I_i is the inertial moment around the CM of i-th link, and a_i is the distance from a joint to the CM of the i-th link in a positive direction toward a distal joint.

Figure 4 shows the model used in simulation. Generalized coordinates $\boldsymbol{\xi}$ are as follows:

$$\boldsymbol{\xi} \ (\ _{1} \cdots \ _{17,} X, Y, \ _{m1} \cdots \ _{m4})^T \quad . \ . \ . \ (1)$$

where

$_{1,} \cdots, \ _{17}$: absolute angles of each link

X, Y: coordinates of the back end of a link of the body

$_{m1}, \cdots, \ _{m4}$: rotational angles of motors for the fetlock drive

We introduced following 4 constraints $\boldsymbol{\Phi}(\boldsymbol{\xi})$=0.

1. Tarsal movement is linked to movement of the stifle by a closed link (this constraint is continuously applicable).
2. The leg is fixed at one point on the ground during the support phase (if the vertical coordinate of a swinging leg y is y 0, this constraint holds true. If the vertical component of floor reaction of a supporting leg $_{vi}$ is $_{vi}$ 0, this constraint does not hold true).
3. Constraint due to the relationship between the angle of the fetlock and the rotational angle of a motor for the fetlock drive (**Fig.5**). This constraint holds true under conditions (a) and (b) in **Fig.5**).
4. Constraint due to the limitation of the rotational angle of the fetlock (if the fetlock angle became limited by a stopper, this constraint holds true. If the reaction from the stopper became zero or less, this constraint does not hold true).

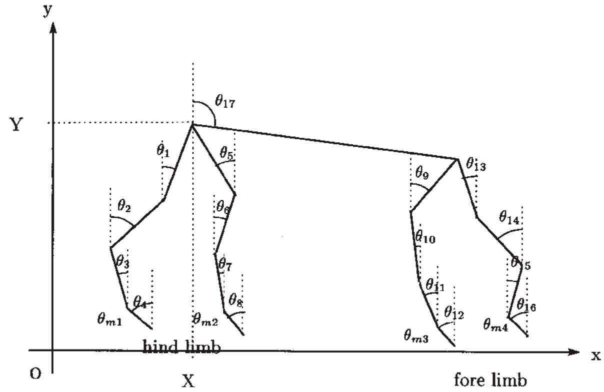

Fig. 4. Generalized coordinates.

Table 3. Foreleg.

	$l_i[m]$	$m_i[kg]$	$I_1[Nm^2]$	$a_i[m]$
Upper arm	0.11	1.720	0.0035	-0.05
Forearm	0.175	1.568	0.0017	0.06
Metacarpus	0.117	1.583	0.0031	-0.01
Digit	0.10	0.294	0.0004	0.05

Table 4. Hind leg and body.

	$l_i[m]$	$m_i[kg]$	$I_1[Nm^2]$	$a_i[m]$
Thigh	0.12	1.769	0.0035	-0.05
Tibia	0.22	0.451	0.0017	0.10
Metatarsus	0.13	1.573	0.0031	-0.03
Pedal	0.10	0.294	0.0004	0.05
Body	0.60	11.062	0.0170	0.30

Table 5. Reduction ratio and motor inertia.

Reduction ratio			
Shoulder	90.2	Hip	90.2
Cubitus	75.4	Stifle	90.2
Carpus	50.0	Tarsus	—
Fetlock (fore)	34.5	Fetlock (hind)	34.5
Motor inertia : $0.11 \times 10^{-5}[N \cdot m^2]$			

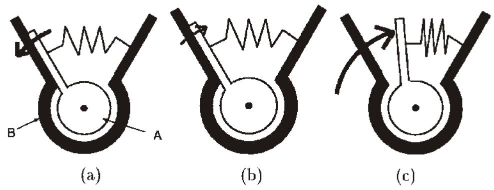

Fig. 5. Conceptual diagram of motor--spring mechanism.

3.2. Equation of Motion

We adopted the generalized coordinates in the previous section. The equation of motion of this system is given by

$$A(\xi)\ddot{\xi} \quad \boldsymbol{B}(\xi,\dot{\xi}) \quad D\boldsymbol{T} \quad E\boldsymbol{\Lambda} \quad . . . . \quad (2)$$

where

$$E \quad \left(\frac{\boldsymbol{\Phi}(\xi)}{\xi}\right)^{T} \quad . . . . \quad (3)$$

where $A(\xi)$ is an inertial matrix, $\boldsymbol{B}(\xi,\dot{\xi})$ is a vector concerned with centripetal force and gravity, D is an input matrix, $\boldsymbol{T}$ is a vector of input torque, and $\boldsymbol{\Lambda}$ is a vector of undetermined multipliers.

Multipliers for each constraint correspond to force or torque occurring under each constraint. When, for example, the *i*-th leg is a supporting leg, undetermined multipliers $_{vi}$ and $_{hi}$ correspond to vertical and horizontal components of the floor reaction .

The torque due to displacement of a spring for the fetlock drive is considered in the first term on the right side of eq. (2).

We also assumed that impulsive force acts when the leg contacts the floor in simulation. If all the constrains of this system just as the leg contact are represented $\boldsymbol{\Phi}_p(\xi)$ 0, then Lagrange's equation of motion for impulsive force is given as

$$A\dot{\xi} \quad A\dot{\xi} \quad E_p\boldsymbol{\Lambda}_p\,,\ E_p \quad \left(\frac{\boldsymbol{\Phi}_p(\xi)}{\xi_p}\right)^{T} \quad . . . \quad (4)$$

where $\dot{\xi}$ is a vector of generalized velocity just after contact $\dot{\xi}$, is a vector of generalized velocity just before contact, and $\boldsymbol{\Lambda}_p$ is a vector of constraint forces including impulsive force that fixes the leg at a point on the floor. From constraints $\boldsymbol{\Phi}_p(\xi)$ 0 and eq.(4), the vector of generalized velocity just after contact is given as

$$\dot{\xi} \quad I \quad A^{1}E_p(E_p^T A^{1}E_p)^{1}E_p^T \quad \dot{\xi} \quad . . . \quad (5)$$

If the leg contacts the floor, we solve eq.(5) to get $\dot{\xi}$, then use generalized velocities as initial conditions and solve the equation of motion by the Runge-Kutta-Gill method.

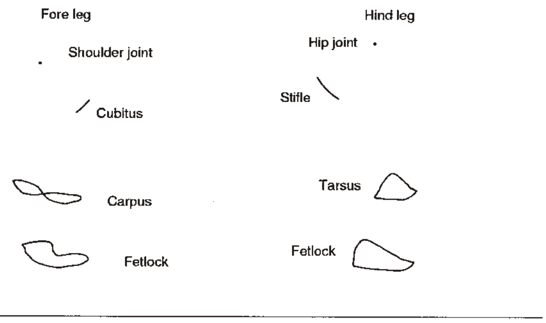

Fig. 6. Target trajictories for each joint.

4. Simulation

4.1. Reference Trajectories

One purpose of this study is to realize a horse-like gait with a quadruped robot. The reference angle of each joint in simulation was based on trot analysis data. We made reference angles by downsizing this data to match PONY. The reduced ratio was one-third vertically and one-sixth horizontally. Based on simulation, we used the same time scale as for the horse because motors were saturated and could not follow references. We used the horizontal reduced ratio because of the saturation of motors and limitations of each joint angle.

When setting reference angles for joints, we focused on the angles of a digit (or pedal) part, and the relative angles between a metacarpal (or metatarsal) part and a digit (or pedal) part, because a spring for the fetlock drive of PONY acts as the tendon's elastic element at the equine fetlock.

The reference angle of upper joints was obtained by calculating inverse kinematics and we adopted angles that bend opposing legs at the cubitus and stifle. This trajectory was based on trot analysis data, and differs from a completely symmetrical trajectory based on robot engineering.

4.2. Control

Each joint was controlled by PD control. The reference trajectories in the previous section are given for joints other than the fetlock.

Fetlock control differs from that for other joints, using a spring serially connected to a motor in the fetlock drive (**Fig.5**). This spring was deformed by 20°.

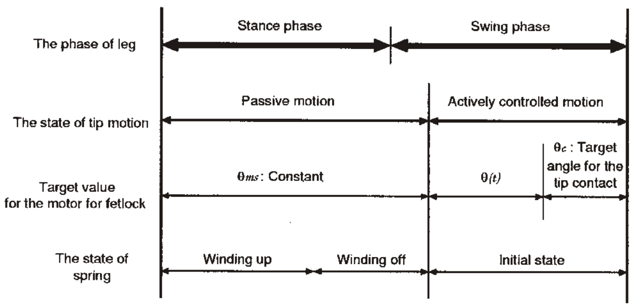

Fig. 7. Control method for fetlock.

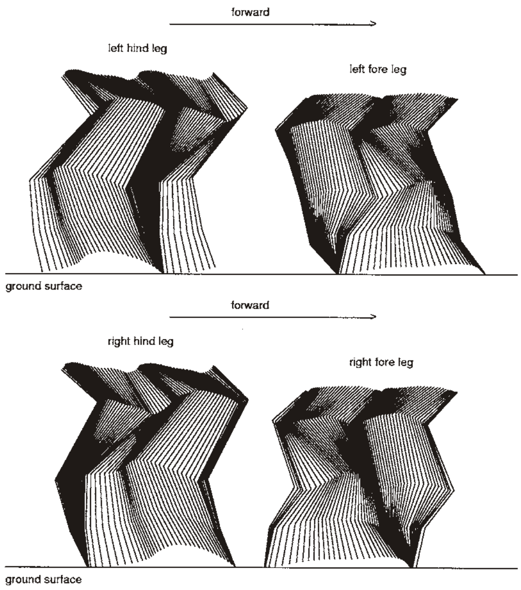

Fig. 9. Stick diagram.

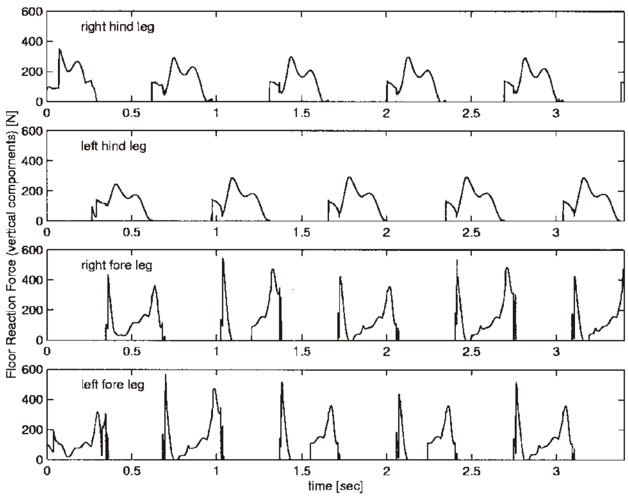

Fig. 8. Reaction force from floor; Virtical components.

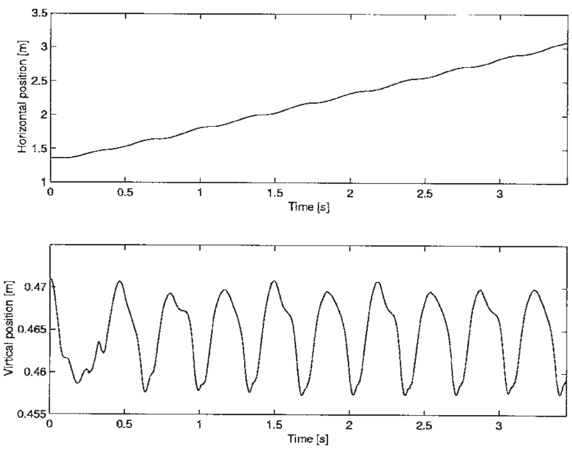

Fig. 10. Center of mass of body.

Because of this initial angle of 20°, the spring underwent constant initial pressure. Thus, if the input axis indicated by A in **Fig.5** generated counterclockwise torque (**Fig.5(a)**) or the input axis indicated by A generated clockwise torque smaller than torque caused initial pressure (**Fig.5(b)**), input A is pressed against output B. Torque transmission is therefore not through the spring. **Fig.5(c)** shows input generated clockwise torque greater than the torque caused by initial pressure. In this case, the spring is aligned between input and output. The fetlock was controlled asshown in **Fig.7** in two phases:

1. Passive motion phase (from the beginning of the support phase to when the spring returns to its initial angle of 20). During this phase, one constant reference angle (the rotational angle of the motor when the leg contacts the floor) is given for the motor. Thus only the spring acts in the movement of the fetlock. Movement is controlled passively by the spring, not actively by the motor.
2. Active control phase (from when the spring returns to its initial angle of 20 to the end of the swing

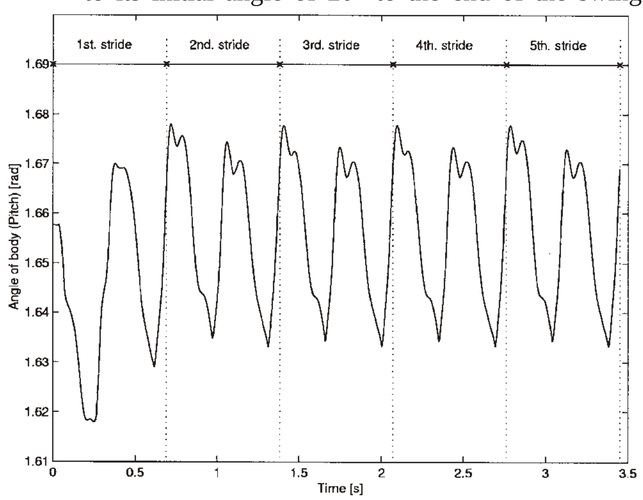

Fig. 11. Pitch angle of body.

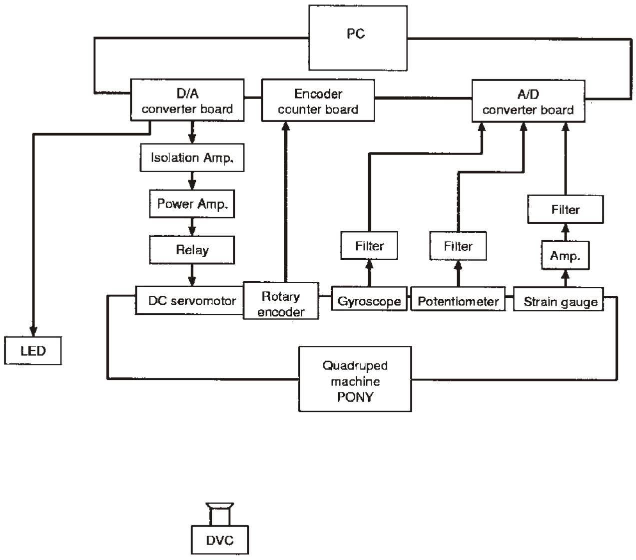

Fig. 12. System of experiment.

phase). During this phase, the drive for the fetlock is considered as a rigid body, and the relationship between the rotational angle of the motor for the fetlock drive $_m$ and the joint angle of the fetlock $_f$ is $_m$ N $_f$, where N is the reduction ratio. The movement of the fetlock is controlled by the motor and follows the reference trajectory.

4.3. Simulation Results

Simulation using the reference trajectory was based on trot analysis data. The following is the result of simulation experiments for 5 complete strides. One complete stride (from setting down of the left foreleg to its next setting down) took about 0.69 seconds. The vertical component of floor reaction is shown in **Fig.8** and indicates that trotting, in which the legs are synchronized on a diagonal line, was achieved. The average duty factor for the foreleg was 0.53 and that for the hind leg 0.51, and the average duty factor for all legs was 0.51.

One complete stride is diagramed in **Fig.9**, which shows the left foreleg and hind leg above and the right foreleg and hind leg below.

Figure 10 shows changes in CM for the horizontal above and for the vertical below. The vertical CM changes within about 0.011[m], while the horizontal CM increases roughly monotonously.

The change in pitch angles is shown in **Fig.11**, which indicates that the gait had two large peaks in rotation around the pitch axis during one complete stride. These results show that this gait has a limit cycle whose period is the same as that of one complete stride (about 0.69 seconds) and the gait is stable.

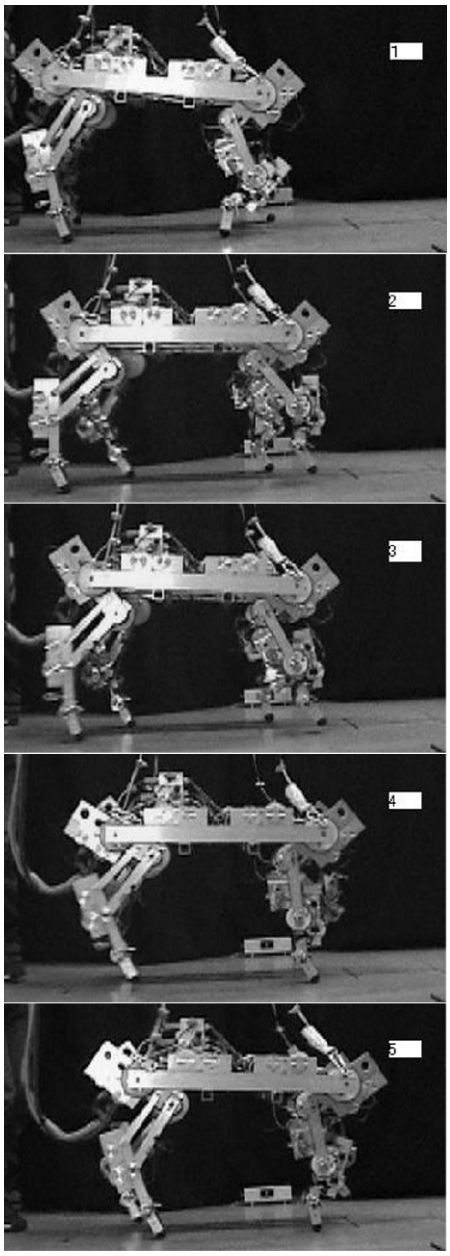

Fig. 13. Trot by PONY; 1 step (From video).

5. Trot Experiment

Using the same reference trajectories and control as for simulation, we conducted a trot experiment using PONY.

5.1. Experimental System

In the experimental system (**Fig.12**), PONY was controlled by an external PC. Power for actuators, etc., was also external and output signals of sensors were transmitted by electrical wires through interface boards.

Since the drive for the fetlock has the mechanism shown in **Fig.5**, we apply initial pressure to the spring. In

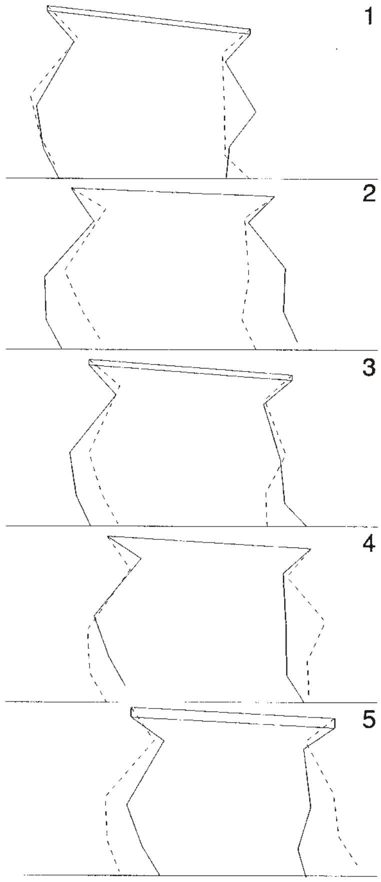

Fig. 14. Stick diagram; 1 step (Experiment).

this experiment, the spring was deformed by 20°, so the torsion angle of the spring for the fetlock drive did not became smaller than 20°.

5.2. Experimental Results

Trot experiments with PONY used reference trajectories based on trot analysis data. The entire experiment was monitored by video imaging of PONY from the side (30[f/s]) (**Fig.13**). The interval between each image is 4 frames (2/15[s]) (**Fig.14**). The right legs are represented by solid lines and the left by broken lines. States 2 and 4 (**Figs.13** and **14**) show that legs on a diagonal line are synchronized, i.e., the gait is a trot. States 1 and 5 show that the left and right legs are synchronized, i.e., the gait is pacing. Because reference trajectories in this experiment were based on equine trot trajectories, this is not completely symmetrical trot based on robot engineering so pacing phase was appeared in the trot.

Figure 15 shows the phase for each leg. Black circles represent the support phase. Dotted lines 1 to 5 represent time corresponding to images 1 to 5 in **Figs.13** and **14**. **Fig.15** shows that the legs on a diagonal line are nearly synchronized. As shown in images from the video pacing phase, the left and right legs were also synchronized. The average duty factor of the forelegs was 0.53 and that of the hind legs 0.54, and that of all legs was 0.53.

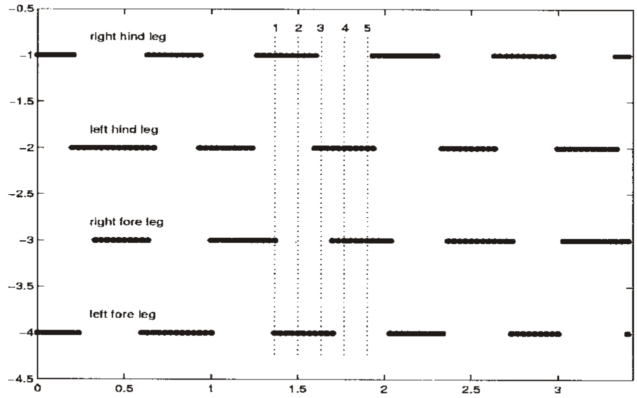

Fig. 15. Leg status.

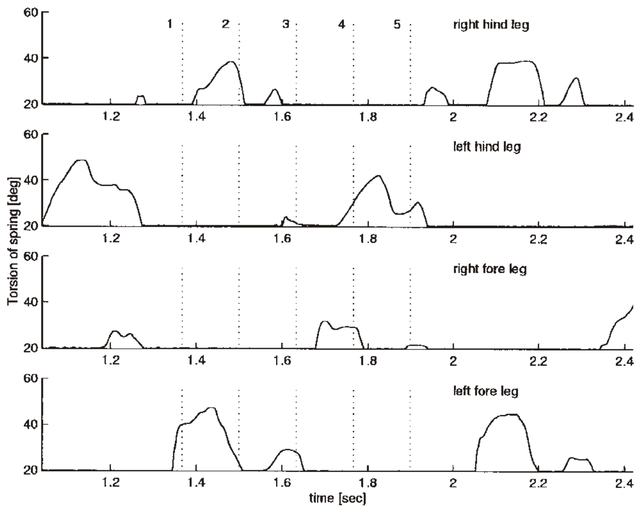

Fig. 16. Torsion angles of springs (Experiment).

The torsion angles of the spring for the fetlock drive are shown in **Fig.16**. Dotted lines 1 to 5 represent time corresponding to images 1 to 5 in Figs. 13 and 14 as in **Fig.15**. Comparing **Figs.15** and **16** shows that in part of the support phase, the torsion angle of the spring for each fetlock drive became larger than its initial angle of 20°. Throughout the support phase, the motor for the each fetlock drive was servolocked, making the torsion angle larger than its initial level only when torque generated in the fetlock by the leg reacting with the floor became larger than initial torque due to the initial torsion angle of the spring. The maximum torsion angle was about 50 . Under this condition, torque around the fetlock generated by the spring for the fetlock drive was about 14[Nm].

6. Summary and Conclusions

A horse-type quadruped robot, PONY, was developed based on equine skeleton data and gait analysis. We reported the development of PONY [24] and studied the following:

1. We developed a simulator to calculate walking movement on the sagittal plane. This simulator had 4 constraints: (1) The leg is fixed at a point on the floor when it comes down; (2) Constraint due to the closed link of the hind leg; (3) Constraint due to the fetlock drive mechanism; (4) Constraint due to the limit on the fetlock rotational angle. These constraints are introduced in the equation of motion by Lagrange's undetermined multipliers and switched depending on walking conditions.
2. We made reference trajectories based on equine limb trajectories and examined control using a simulator, achieving control for stable walking.
3. Trot experiments on 5 complete strides were conducted using control and reference trajectories for simulation using PONY, realizing stable trotting.

Acknowledgments
We thank the Equine Research Institute, Japan Racing Association (JRA), for equine data and Dr. Makoto Kai for his helpful advice and commen.

References:

[1] R. B. McGhee, and A. A. Frank, "On the stability Propertes of Quadruped Creeping Gaits, Mathematical Biosciences", Vol.3, pp. 331-351, 1968.
[2] J. Furusho, "Evolution of Research on Legged Locomotion -Perspective of Special Issue on Walking Robot-", J. of the Robotics Society of Japan, Vol.11, No.3, pp. 306-313, 1993.
[3] M. H. Raibert, M. Chepponis and H. B. Brown, Jr. , "Running on Four Legs As Through They were One", IEEE Journal of Robotics and Automation, Vol.RA-2, No.2, pp.70-82, 1986.
[4] H. Mirura, I. Shinoyama, M. Mitsuishi, and H. Kimura, "Dynamical Walk of Quadruped Robot'', Cambridge, MA, MIT Press, 1985.
[5] H. Kimura, I. Shimoyama, H. Mirura, "Dynamics and Control of the Quadruped Robot Dynamic Walk by use of the Redundancy of Actuators Caused by the Multiple Touching Legs", Transactions of the Japan Society of Mechanical Engineers, 1995), Vol.55, No.517, pp. 2396-2410, 1995.
[6] S. Hirose, K. Yoneda, "Dynamic & Static Fusion Control and Continuous Trajectory Generation of Quadruped Walking Robot", J. of the Robotics Society of Japan , Vol.9, No.3, pp. 267-275, 1991.
[7] R. Kurazume, A. Haishi, K. Yoneda, S. Hirose, "Stabilizing Control for Dynamically Stable Walking of Quadruped Walking Robot", J. of the Robotics Society of Japan , Vol.19, No.3, pp. 380-386, 2001.
[8] T. Emura and A. Arakawa, "Attitude Control of a Quadruped Robot during Two Leg Supporting", Proc. 5th Int. Conf. Advanced Robotics, Piza, pp. 711-716, 1991.
[9] Y. Sakakibara, K. Kan, Y. Hosoda, M. Hattori, M. Fujii, "Low Impact Foot trajectory for a Quadruped Walking Machine", J. of the Robotics Society of Japan , Vol.8, No.6, pp. 662-671, 1990.
[10] Y. Takita and K. Seto, "The Semi-Dynamical Walking of a Quadruped Robot", Proc. USA-JAPAN Symp. Flexible Automation, pp. 681-686, 1988.
[11] S. Akiyama, H. Kimura, "Dynamic Quadruped Walk Using Neural Oscillators Realization of Pace and Trot" Proceedings of The 13 th Annual Conference of RSJ, pp.227-228, 1995.
[12] H. Kimura, K. Sakurama and S. Akiyama, "Dynamic walking and running of the quadruped using neural oscillator", Proc. Int. Conf. Intelligent Robots and Systems (IROS '98), 1998.
[13] Y. Fukuoka, H.Kimura, "Biologically Inspired Adaptive Dynamic Walking of a Quadruped Robot on Irregular Terrain Adjustment based on somatic sensation and vestibular sensation", J. of the Robotics Society of Japan, Vol.19, No.4, pp. 510-517, 2001.
[14] G. Hawker, and M. Buehler, "Quadruped Trotting with Passive Knees-Design, Control, and Experiments", Proc. IEEE International Conference on Robotics and Automation, pp. 444-449, 2000.
[15] D. Papadopoulos, and M. Buehler, "Stable Runnning in a Quadruped Robot with Compliant Legs'', Proc. IEEE International Conference on Robotics and Automation, pp. 3046-3051, 2000.
[16] J. Furusho, A. Sano, M. Sakaguchi and E. Koizumi, "Realization of Bounce Gait in a Quadruped Robot with Articular-joint-type legs", Proc. IEEE International Conference on Robotics and Automation, Vol.1, pp.697-702, 1995.
[17] A. Sano, J. Furusho, S. Ozeki, "A Pace Gait of Quadruped Robot Based on The Control of Walking Cycle Using A Discrete-time Model", J. of the Robotics Society of Japan , Vol.9, No.7, pp. 865-876, 1991.
[18] A. Sano, J. Furusho, "Static-Dynamic Transitional Gait from Crawl to Pace'', Proceedings of JASME Annual Conference on Robotics and Mechatronics '92 , Vol.B, pp.239-242, 1992.
[19] H. Takeuchi, "Development of MEL HORSE", Proc. IEEE International Conference on Robotics and Automation, pp. 1057-1062, 1999.
[20] Septimus Sisson, revised by J. D. Grossman, "The Anatomy of the Domestic Animals'' [4th ed.], Modern Asia Edition, 1961.
[21] Yoshitaro Kato, Shoji Yamauchi, ''Illustrated Dictionary of Comparative Anatomy of Livestock", Yokendo, Revised 1995.
[22] K. Kubo, T. Sakai, H. Sakuraoka, and K. Ishii, "Segmental Body Weight", Volume and Mass Center in Thoroughbred Horses, Jpn. J. Equine Sci., Vol.3, No.2, pp. 149-155, 1992.
[23] Toshiro Kamiya, ''Zoology of Bones'', University of Tokyo Press, 1995.
[24] S. Makita and J. Furusho, "Development of Horse-type Quadruped Robot -Report 1, Development of Mechanism and Control System of Quadruped Robot PONY-", J. of Robotics and Mechatronics, Vol.15, No.4, pp. 442-450, 2003.

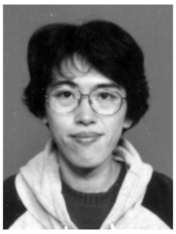

Name:
Shinobu Makita

Affiliation:
International Rescue System Institute

Address:
Kobe KIMEC Center Bldg. 2F, 1-5-2 Minatojima, Minami Machi, Chuo-ku, Kobe 650-0047, Japan

Brief Biographical History:

1992- ASICS Corp.

1994- Tokyo Metropolitan University

1997- Osaka University

2003- International Rescue System Institute

Main Works:

"Consideration of Evaluation of Robot Arm Mechanism", S. Makita and J. Furusho, J. of the Robotics Society of Japan, Vol.20, No.7, pp.742-750, 2002.

Membership in Learned Societies:

The Japan Society of Mechanical Engineers (JSME)

The Robotics Society of Japan (RSJ)Name:

Name:
Daisuke Nishimura

Affiliation:
Matsushita Electric Works, Ltd.

Address:
1048 Kadoma, Osaka 571-8686, Japan

Brief Biographical History:
2001- Matsushita Electric Works, Ltd.

Main Works:

"Control of Horse-type Quadraped Robot (Experiment and Simulation)", D. Nishimura, S. Makita, T. Kodera, M. Hisano, N. Takesue, M. Sakaguchi and J. Furusho, Proc. of SICE Kansai Chapter 2000, 2000.

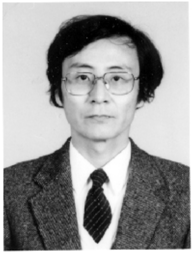

Name:
Junji Furusho

Affiliation:
Professor, Department of Computer-Controlled Mechanical Systems, Graduate School of Engineering, Osaka University

Address:
2-1 Yamadaoka, Suita, Osaka 565-0871, Japan

Brief Biographical History:
1976- Research Associate at Osaka University
1982- Associate Professor at Gifu University
1991- Professor at the University of Electro-Communications
1996- Professor at Osaka University

Main Works:

Control theory and Process Control (1975-1985)

Biped robot and quadruped robot (1980-2003)

Intelligent artificial legs

Rehabilitation training systems

Haptic devices and virtual reality

Power assist systems and human friendly robotics

New mechatronics using intelligent fluids

Motion control of mechatronics systems

Surgical robots

Membership in Learned Societies:

The Japan Society of Mechanical Engineers (JSME)

The Robotics Society of Japan (RSJ)

The Society of Instrument and Control Engineers (SICE)

The Virtual Reality Society of Japan (VRSJ)

Society of Biomechanism Japan (SOBIM)

The Institute of Electrical Engineers of Japan (IEEJ)